

This discussion paper is/has been under review for the journal Atmospheric Chemistry and Physics (ACP). Please refer to the corresponding final paper in ACP if available.

The effect of low solubility organic acids on the hygroscopicity of sodium halide aerosols

L. Miñambres, E. Méndez, M. N. Sánchez, F. Castaño, and F. J. Basterretxea

Departamento de Química Física, Facultad de Ciencia y Tecnología, University of the Basque Country, UPV/EHU, Campus de Leioa, B. Sarriena, s/n, Leioa 48940, Spain

Received: 28 November 2013 – Accepted: 24 January 2014 – Published: 18 February 2014

Correspondence to: L. Miñambres (lorena.minambres@ehu.es)

Published by Copernicus Publications on behalf of the European Geosciences Union.

4383

Abstract

In order to accurately assess the influence of fatty acids on the hygroscopic and other physicochemical properties of sea salt aerosols, hexanoic, octanoic or lauric acid together with sodium halide salts (NaCl, NaBr and NaI) have been chosen to be performed in this study. The hygroscopic properties of sodium halide submicrometer particles covered with organic acids have been examined by Fourier-transform infrared spectroscopy in an aerosol flow cell. Covered particles were generated by flowing atomized sodium halide particles (either dry or aqueous) through a heated oven containing the gaseous acid. The obtained results indicate that gaseous organic acids easily nucleate onto dry and aqueous sodium halide particles. On the other hand, Scanning Electron Microscopy (SEM) images indicate that lauric acid coating on NaCl particles makes them to aggregate in small clusters. The hygroscopic behaviour of covered sodium halide particles in deliquescence mode shows different features with the exchange of the halide ion: whereas the organic covering has little effect in NaBr particles, NaCl and NaI covered particles change their deliquescence relative humidities, with different trends observed for each of the acids studied. In efflorescence mode, the overall effect of the organic covering is to retard the loss of water in the particles. It has been observed that the presence of gaseous water in heterogeneously nucleated particles tends to displace the cover of hexanoic acid to energetically stabilize the system.

1 Introduction

Marine aerosol is one of the most abundant types of natural particulate matter in the Earth's troposphere. Sea salt particles play an active role in the Earth's radiative balance, influence mass transfer from gaseous substances and cloud-precipitation mechanisms, contribute to the formation of cloud condensation nuclei and have highly reactive surfaces that take part in heterogeneous and multiphase chemical reactions

4384

(Andreae and Rosenfeld, 2008; Carslaw et al., 2010; O'Dowd and De Leeuw, 2007; Finlayson-Pitts, 2003; Lewis and Schwartz, 2004; Quinn and Bates, 2011; Rossi, 2003). They also can uptake significant amounts of water, exhibiting deliquescence and efflorescence properties under atmospheric conditions (Freney et al., 2009; Martin, 2000; Metzger and Lelieveld, 2007; Mikhailov et al., 2013; Wise et al., 2012), that can change the particles' phase and other physico-chemical properties. Although sodium chloride is the principal component of sea salt, several studies indicate that minor components, such as bromide and iodide ions, exhibit a higher surface reactivity than chloride. This is due to the tendency of Br^- and I^- to segregate to the salt surface in the presence of water, substantially increasing Br/Cl and I/Cl surface molar ratios (Baker, 2005; Ghosal et al., 2008; Zangmeister et al., 2001). Bromine and iodine play active roles in tropospheric sea salt chemistry and are involved in tropospheric and stratospheric ozone destruction (Finlayson-Pitts, 2009; Frinak and Abbatt, 2006; Hunt et al., 2004; Saiz-Lopez et al., 2007; Von Glasow, 2008). Recently advances have been made in quantifying the link between seawater chemical processes, and the production, size, and chemical composition of sea spray aerosol particles (Prather et al., 2013).

Organic compounds are present in marine salt aerosol in variable proportions, that may represent a large fraction of the aerosol dry mass (Cavalli et al., 2004; Gantt and Meskhidze, 2013; Middlebrook et al., 1998). Much of the organic fraction corresponds to water insoluble fatty acids present as surface films on particles (Donaldson and Vaida, 2006; Mochida et al., 2002; Tervahattu et al., 2002). It has been proposed that the organic compounds arrange in a hydrophobic organic monolayer that encapsulates an aqueous particle, forming an "inverted micelle" structure (Ellison et al., 1999). This model shows agreement with recent molecular dynamic simulation results (Chakraborty and Zachariah, 2008). Other models predict that certain fatty acids form pockets of micelles within the aerosol (Tabazadeh, 2005), and that core-shell structures are not always the most stable (Kwamena et al., 2010). The presence of an organic film at the surface of a particle may affect its physical and chemical properties in a number of ways. The film may act as a barrier to transport across the

4385

interface, inhibiting uptake of atmospheric gases or reaction (Donaldson and Vaida, 2006). In particular, the surface film can affect the process of cloud condensation nuclei formation and growth (Andrews and Larson, 1993; Chuang, 2003) and also change the hygroscopic properties of marine aerosols. In general, there is much uncertainty about fundamental issues of marine primary organic aerosol (POA), such as chemical composition, mixing state, hygroscopicity, cloud droplet activation, formation, aging and removal mechanisms (Carslaw et al., 2010; O'Dowd and De Leeuw, 2007; Gantt and Meskhidze, 2013). Recent results indicate that the ambient mass concentration and organic mass fraction of sea-spray aerosol are related to surface ocean biological activity, and that, marine POA can cause large local increases in the cloud condensation nuclei concentration. Moreover, fine POA can have a size distribution independent from that of sea-salt, while coarse mode aerosols are more likely to be internally mixed with sea-salt (Gantt and Meskhidze, 2013). Several laboratory studies about the effect of organic surfactants, such as palmitic and oleic acids, on NaCl , ammonium sulfate or mineral dust aerosol particles as a function of relative humidity have been reported employing a variety of experimental techniques, such as electrodynamic balance, infrared spectroscopy, electrical mobility, optical tweezers, cavity ring-down spectroscopy or nonlinear spectroscopy (Cwiertny et al., 2008; Davies et al., 2013; Dennis-Smith et al., 2012; Ebben et al., 2013; Garland et al., 2005; Hansson et al., 1998; Najera and Horn, 2009; Robinson et al., 2013; Rossi, 2003; Rubasinghege et al., 2013). The general conclusions are that hygroscopic growth, deliquescence relative humidity (DRH) and efflorescence of the particles may be affected by several factors, such as coating thickness or structural arrangement of the organic film. Special effort has been carried out to study the morphology and phase partitioning of aerosol particles consisting of hydrophobic and hydrophilic phases (Ciobanu et al., 2009; Kwamena et al., 2010; Reid et al., 2011; Veghte et al., 2013). On the other hand, molecular dynamics calculations are becoming a commonplace theoretical approach in atmospheric aerosol modelling, that includes sea salt particles mixed with organic molecules (Ma et al., 2011; Sun et al., 2012, 2013; Takahama and Russell, 2011).

4386

As a whole, laboratory studies on inorganic particles coated with surfactant organics have mainly focused on a few organic molecules, and most of them have been carried out with ammonium sulfate or sodium chloride. Very few studies of hygroscopic behavior have been carried out on particles containing bromide or iodide. Furthermore, sodium chloride, bromide and iodide particles exhibit very different hygroscopic properties and interact differently with water soluble dicarboxylic acids such as succinic acid (Minambres et al., 2011). It has been reported that rates of gaseous iodine emissions during the heterogeneous reaction of O_3 with interfacial iodide are enhanced several-fold by the presence of alkanolic acids on water, such as octanoic and hexanoic acid (Hayase et al., 2011). In the present work we study the hygroscopic properties of NaX ($X = Cl, Br, I$) sodium halide salts coated with either one of three different surfactant carboxylic acid molecules by Fourier-transform infrared extinction spectroscopy in an aerosol flow tube, aided by particle sizing methods. The examined acids, all contain one carboxylic group at the end of the molecule, are hexanoic ($CH_3(CH_2)_4COOH$), octanoic ($CH_3(CH_2)_6COOH$) and lauric acid ($CH_3(CH_2)_{10}COOH$), hereafter shortened as HA, OA and LA, respectively. Infrared spectroscopy is a well-known sensitive technique and has been applied to the study of organic/inorganic aerosol systems (Garland et al., 2005; Najera and Horn, 2009). It can yield aerosol composition, water content, and particle phase. Variations in the wavenumbers and widths of spectral bands can also reveal information about molecular interactions in mixed systems and the formation of new species. Infrared spectra have been combined with electron scanning microscopy (SEM) of particles, a technique that has been demonstrated to be useful to study the chemistry of isolated, individual particles of atmospheric relevance (Krueger et al., 2003; Veghte et al., 2013). Octanoic and lauric acids exist as liquid and solid, respectively, at typical tropospheric temperatures and pressures, and have been observed in the atmosphere of remote marine and continental locations (Duce et al., 1983; Gill et al., 1983). Finally, hexanoic acid is intermediate between soluble and highly insoluble organic acids, and has higher vapor pressures than the atmospherically more abundant long chain acids, that may contribute more substantially to

4387

vapor phase processes. A few studies have been presented describing the effects of octanoic and lauric acids on the hygroscopicity of NaCl (Hämeri et al., 1992; Hansson et al., 1998; Wagner et al., 1996). The results indicate that formation of organic surfactant layers tend to slow NaCl deliquescence rate and to slightly lower its DRH. Molecular dynamics simulations of water vapor molecules impinging on a slab of water coated by octanoic acid film showed that the mass accommodation coefficient decreased with the degree of surface coverage of the hydrocarbon backbones (Takahama and Russell, 2011).

2 Materials and methods

The configuration of the experimental setup used in this work is based on a system described previously (Minambres et al., 2010), that has been modified for the present study. The main elements are depicted in Fig. 1.

Submicrometric particles are formed by injecting a 0.01 kg L^{-1} aqueous solution of sodium halide salts (NaCl, NaBr and NaI, $\geq 98\%$) in a commercial atomizer (TSI 3076). Their relative humidity (RH) can be controlled (from 0 to around 95%) by combining two serially connected diffusion driers and a flow of N_2 with a controlled amount of water vapor. The inorganic particles are coated by passing the aerosol flow through a heated cell that contains a sample of either hexanoic (99%), octanoic ($\geq 98\%$), or lauric acid ($\geq 98\%$). Table 1 summarises the most relevant physical properties of these acids.

The cell consists of an horizontally-set cylindrical borosilicate glass tube 30 cm long having 3 cm internal diameter, that has two smaller glass tubes (30 and 20 cm long, 1 cm int. diam.) coaxially attached at its ends. Acid sample (either liquid or solid) is placed uniformly along the central tube. The whole cell is thermally isolated by wrapping it with alumino-silicate refractory ceramic fiber. To allow for sufficient vaporization of the acid, the central tube and exit arm of the cell are heated up to 100°C by means of flexible resistors coiled around them. The temperatures at both cell locations (T_1 refers

4388

to the central part, T_2 to the exit arm, see Fig. 1) are controlled by placing two K-type thermocouples at the cell outer walls. To form heterogeneously nucleated particles, T_1 varied from 75 to 100 °C and T_2 from 60 to 90 °C. Higher temperatures resulted in stronger absorption bands, indicating a higher efficiency of heterogeneous nucleation, that forms a thicker coating of NaCl particles. A prominent baseline shift was observed in all cases, in agreement with particle formation. This shift increases with T_1 and T_2 , indicating bigger particles. Purely homogeneously nucleated particles were formed by passing a flow of gaseous nitrogen through the heated oven at $T_1 = 80\text{--}100$ °C and $T_2 = 60\text{--}90$ °C containing the carboxylic acid.

The final aerosol flux was directed simultaneously to a condensation particle counter (CPC, either TSI 3781 or MSP 1040XP models), an aerodynamic particle spectrometer (APS, TSI 3321) and a Fourier-transform infrared spectrometer (Nicolet Magna 860), to obtain particle number, size distribution and their infrared extinction spectra, respectively. Particle size distribution in the 0.5–20 µm is retrieved by an aerodynamic particle spectrometer (TSI 3321), that give a tail in the 0.5–3.5 µm range. Information about the size distribution of pure salt particles in the 0–0.5 µm range was obtained by measuring the infrared scattering spectrum of dry NaBr particles (taken as representative of solid salt) and comparing it to the predicted Mie scattering spectrum (Bohren and Huffman, 2004), that was computed assuming a lognormal distribution of particles with given values of average diameter, geometric standard deviation, and total particle number density (Minambres et al., 2008). Optical constants for NaBr were taken from the literature (Li, 1976). In this way, a value of median diameter of 0.3 µm and standard deviation of 1.29 was obtained that best fitted the measured scattering spectrum and the particle size distribution.

To complete analytical on-line methodology, particle shape and size of both pure and mixed particles were determined off-line using a JEOL JSM-7000F scanning electron microscope (SEM), equipped with a Schottky field emission gun (FEG) and an Oxford Inca Pentafet X3 energy dispersive X-ray analyser (EDX). The EDX microanalysis was performed using an accelerating voltage of 20 kV and a current intensity of 10^{-10} A,

4389

with a working distance of 10 mm. The aerosol of interest was collected at the exit of the extinction flow cell onto a glass slide, and particles were coated with an Au layer (20 nm) deposited by evaporation using a Quorum Q150T Sputter Coater to provide electrical conductivity.

3 Results and discussion

3.1 Infrared spectra of pure carboxylic acids

The infrared absorption spectra of bulk HA, OA and LA recorded at ambient temperature are presented in Fig. 2. The spectra of HA and OA were recorded in an infrared cell for liquids, whereas for LA one drop of the sample dissolved in ethanol was deposited on a BaF₂ window until solvent evaporation, after which the absorption spectrum of the film was recorded. The main absorption bands are common to all three acids, with small differences in band position and intensity.

The sharp carbonyl stretching band outstands near 1710 cm⁻¹, the broad band in the 2500–3500 cm⁻¹ range has been assigned to associated COO–H stretchings (broadened by intermolecular association by hydrogen bonding), whereas the group of three peaks in the 2800–3000 cm⁻¹ range, exhibiting a different resolvable structure for the different acids, has been assigned to –C–H stretchings. A more complex band system appears in the 800–1500 cm⁻¹, specific of each acid. On the other hand, the gas phase infrared spectra of the three acids (NIST Chemistry Webbook: <http://webbook.nist.gov/chemistry>, not shown in Fig. 1) show several differences with the bulk phase spectrum: the intense C=O band locates in the 1780–1790 cm⁻¹, whereas a narrow band appears near 3580 cm⁻¹ (COO–H free stretch), absent in the condensed phase. Overlapped bands appearing in the 2800–3000 cm⁻¹ range are co-incident with peak positions in bulk phase spectra. Finally, a number of bands is present in the 800–1600 cm⁻¹ region, several of which can be distinguished from condensed phase spectra.

4390

Figure 2 also shows the extinction spectra of homogeneously nucleated particles. Bands belonging to each acid were detected in all cases, their absorption intensity growing with increasing T_1 and T_2 . The presence of carboxylic acid particles was confirmed by CPC measurements. For HA, the obtained spectra are mostly coincident with the gas phase spectrum. A weak band located at near 1730 cm^{-1} has been assigned to the C=O stretch originating from small particles of liquid HA due to homogeneous nucleation. This band is 21 cm^{-1} displaced to higher wavenumbers with respect to bulk liquid HA, possibly due to surface effects in small particles. This hypothesis is supported by the spectrum of liquid HA adsorbed at the air/water interface by vibrational sum-frequency spectroscopy (Soule et al., 2007), that locates the C=O band in the $1726\text{--}1730\text{ cm}^{-1}$ range, depending on the polarization conditions. For OA, the C=O band was peaked at near 1700 cm^{-1} , but broader than the one corresponding to condensed phase. Also an overlapping band system in the $1540\text{--}1650\text{ cm}^{-1}$ range was observed. No lines of gaseous OA were detected. For LA, no gas band features were present, in accordance with its low vapor pressure. Additionally, the spectrum baselines increase slightly to higher wavenumbers as T_2 increases, which is indicative of particle scattering (Hinds, 1998). A broad band in the $3100\text{--}3500\text{ cm}^{-1}$ range is observed for homogeneously nucleated hexanoic and octanoic acid, that is absent in the bulk spectrum. This feature has been attributed to the presence of small amounts of liquid water outgassed from the acid that become trapped into the particles.

The most notable differences in band wavenumber and bandwidth for the three acids are observed for the C=O stretching band, and are summarised in Table 2. These differences can be significant, as can be related with surface effects that can give information about the particles. Carbonyl bandwidth in the bulk acids is in the $20\text{--}29\text{ cm}^{-1}$ range, and increases with molecular mass. These values change in homogeneously nucleated organic particles, either increasing (HA and OA) or decreasing (LA). Relative variations in its magnitude are in the 25–75 % range.

4391

3.2 Infrared extinction spectra of heterogeneously nucleated NaX particles with carboxylic acids

Representative infrared extinction spectra of heterogeneously nucleated sodium halide particles are shown in Fig. 2. The band intensities of heterogeneous nucleation spectra are much bigger than those of homogeneous nucleation (e.g., 4 : 1 for NaCl/OA at $T_1 = 90^\circ\text{C}$, $T_2 = 80^\circ\text{C}$). For NaX/HA particles, bands of gaseous and condensed phase HA were observed. The latter increase in intensity with T_1 and T_2 , whereas the former remain constant. For NaX covered with OA or LA, practically all infrared bands originate from condensed phase, gas phase OA bands being very weak or absent. Their observed carbonyl absorption band wavenumber and bandwidth for the various acids are collected in Table 2. The changes in these magnitudes with respect to their bulk phase values are indicative of organic molecule/inorganic ion interactions, and can be used to address the effect of the ionic salt environment near the organic acid molecules. For all acids, the C=O stretch wavenumber of the acid coating on NaX varies with the salt and is between the wavenumber of the corresponding bulk acid and that of homogeneously nucleated acid particles (Table 2). In all cases, bulk wavenumber of C=O locates around 70 cm^{-1} lower than in the gas phase, bulk LA showing the lowest wavenumber (1700 cm^{-1}). On the other hand, the bandwidths of the C=O stretch coming from heterogeneously nucleated particles depend on the nature of the salt, the organic acid and the degree of covering: for HA-covered particles, the full width half-maximum (FWHM) can reach 40 cm^{-1} , doubling the bulk HA value, whereas for LA-coated particles it is smaller than the bulk acid bandwidth. The relationship of these results with the hygroscopic properties of particles will be discussed later.

3.3 Morphology of pure and mixed particles

SEM images of pure NaCl and LA particles, and of NaCl particles after covering them with LA, were recorded and are presented in Fig. 3. This technique was not well suited to study particles that included OA or HA, due to their high vapor pressure at room tem-

4392

perature that diffculted their manipulation in the SEM vacuum chamber. Images of dry NaCl show cubic particles as expected (see Fig. 3a). The number size distribution of particles was obtained by processing the SEM image with the help of the ImageJ software [rsbweb.nih.gov/ij/]. The obtained distribution fitted satisfactorily to a lognormal distribution with a count median diameter of 46 nm and sigma = 2.0. Particles appear mostly isolated, without a tendency to aggregate.

Images of LA particles (Fig. 3b) show a much smaller amount of particles that tend to form big aggregates, typically of 1–2 μm length, in accordance with previous studies (Gadermann et al., 2008). The particles are amorphous and mostly elongated. Images of NaCl particles deposited jointly with LA (after heterogeneous nucleation, see Fig. 3c) show a small number of particles, much fewer than in the case of pure NaCl, although the initial amount of NaCl aerosol was identical in both cases (this may be due to the low affinity of the mixture with the supporting material or to higher tube losses). Most particles present cubic form, and tend to appear as aggregates. Although pure LA particles can be observed, they are very scarce. A thin layer covering the NaCl particles can be observed, smaller NaCl particles appearing with a thicker covering. Thus it can be said that a thin layer of lauric acid is deposited on NaCl particles, acting as a glue that tends to link individual NaCl particles.

3.4 Deliquescence and efflorescence of heterogeneously nucleated NaX particles with HA, OA and LA

3.4.1 Infrared spectra of particles at various RHs

To examine the deliquescence behavior, dry NaX particles coated with each of the carboxylic acids were mixed with a flow of gaseous water at different RHs. As a representative example, Fig. 4 shows three spectra of NaBr particles covered with OA at various RHs. The presence of liquid water can be detected and quantified by the broad band centered at near 3400 cm^{-1} .

4393

In all cases, we paid special attention to the C=O stretching band of the acids, and we analyzed it as a function of RH, organic acid and halide anion measured. In OA/NaX and LA/NaX particles, the carbonyl band absorption intensity of condensed phase acid keeps constant with RH; on the contrary, for NaX/HA particles the band intensities of liquid HA decrease as RH increases, although the intensities of gaseous HA remain unchanged. As an example, Fig. 5 plots the intensity variation of the carbonyl band vs. RH for liquid and gaseous HA in NaBr particles. It can be seen that, while the C=O band intensity of gaseous HA keeps roughly constant with RH, the band intensity for condensed HA lowers at higher RH. The largest decrease was observed in NaBr, and the smallest in NaI. In all salts, the particles retained liquid HA at RHs higher than their DRH. On the other hand, the spectrum baseline also decreases at high wavenumber as RH increases (due to decrease of particle scattering), indicating a thinner coating of the particles.

The efflorescence behavior of coated aqueous NaX particles was investigated by passing NaX aqueous particles along the heated oven containing the carboxylic acid vapor. For all the systems, at RH near saturation the spectra show bands of condensed phase organic acid. The intensity of these bands keeps roughly constant with RH in OA and LA, but liquid HA band intensities decrease notably as RH is reduced (a factor in the range 3–7 from RH $\approx 100\%$ to 27 %, depending on the salt). Figure 5 shows the case for NaBr/HA. Also the scattering signal is decreases with RH, indicating that particles get smaller.

3.4.2 Deliquescence and efflorescence curves

Deliquescence and efflorescence curves were recorded by measuring the integrated absorbance of liquid water in the particles in the $3400\text{--}3600\text{ cm}^{-1}$ range and plotting the values vs. RH. This interval was selected as it is mostly free of interference with nearby absorption spectral features. The scattering component of the liquid water extinction spectrum was removed by subtracting the sloping baseline present at high wavenumbers to obtain integrated absorbances. The results for all the systems are

4394

presented in Fig. 6. The curves for the pure inorganic salts have also been measured and are included in the figure. Hereafter, we describe the effect of the various acids in each of the inorganic salts.

(1) NaCl particles

5

The deliquescence curve of NaCl/HA is very similar to that of pure NaCl particles, that deliquesce at DRH (298 K) = 75.3 % (Tang and Munkelwitz, 1993). No water uptake is detected until near 73 % RH, where particles abruptly become liquid. The quantity of liquid water uptaken by NaCl particles is unaffected by the presence of the HA covering. However, for NaCl/OA and NaCl/LA, particle deliquescence occurs near to 56 % RH, substantially lower than in pure NaCl. These results are in agreement with previous reports in which a slight lowering of the DRH of NaCl was observed when the particles were covered with OA and LA acids (Hansson et al., 1998). In NaCl/OA, the particles uptake more amounts of liquid water than in pure NaCl, whereas the opposite is observed for NaCl/LA. The efflorescence curves for all the three acids locate the ERH close to 40 %, very similar to pure NaCl particles. The curves are coincident in the RH = 20–60 % range, but diverge towards higher RHs. For all acids, particles retain more amounts of water than pure NaCl in the RH = 60–95 %, the amount being in the order LA > OA > HA. Also the amount of HA and OA in the particles decreases as liquid water is removed from them until the ERH is reached, whereas no change in the amount of LA is observed with RH.

10

15

20

(2) NaBr particles

25

According to Fig. 6 data, NaBr/HA particles deliquesce at somewhat higher RH than pure NaBr particles: liquid water in NaBr/HA particles is not detected until 49.6 % RH. This value does not change with the degree of coating, and contrasts with the value of DRH = 37 % for pure NaBr particles (Minambres et al., 2008). On

4395

5

the other hand, OA and LA coverings do not have any effect in the deliquescence behavior of NaBr: the deliquescence curves are practically coincident with those of pure NaBr. Also, the amount of uptaken water is similar than in pure NaBr, except for OA-covered particles, that grow faster for RH > 70 %. Efflorescence curves for all acid covering are very similar to pure NaBr (ERH = 23 %) in the 20–60 % RH (although OA retains slightly more water at all RHs), but at RH > 60 % acid-covered particles retain higher amounts of liquid water than pure NaBr (up to double for NaBr/LA at 90 % RH). Thus the presence of the organic covering causes water loss to happen more gradually than in the pure salt at high RHs.

10

(3) NaI particles

15

20

25

The deliquescence curves of acid-covered NaI particles exhibit substantial differences with respect to the pure salt. Whereas pure NaI particles take up water at all RHs (Minambres et al., 2011), NaI/HA and NaI/LA particles do not uptake water until RH = 16 % and 21 %, respectively. Liquid water is not detected in NaI/OA particles until RH = 75 %. It can be concluded that organic acid covering substantially retards the uptake of water in NaI particles, specially OA. The amount of liquid water in HA and LA-covered particles in the RH = 20–80 % is higher than in pure NaI. The efflorescence curve of NaI/LA is practically coincident with the pure NaI curve in the RH range measured. However, HA-covered particles lose water more gradually, retaining higher amounts of water than pure NaI in the RH = 30–80 % range. Finally, OA-covered particles follow closely the pure salt curve for RH > 80 %, but retain more water at lower RHs. The general tendency is that the presence of acid covering retains more water in the particles, except for LA, which shows little effect.

3.4.3 Discussion of deliquescence and efflorescence processes

The obtained results on the hygroscopicity of sodium halide particles covered with water insoluble organic acids show an overall complex behavior. The deliquescence curves of Fig. 6 indicate that the water uptake process is dependent on both the inorganic salt and the organic acid. Whereas HA, OA and LA have a smaller effect on water uptake of NaBr (only HA slightly retards the DRH), they produce a lowering of the DRH in NaCl respect to the pure salt. On the contrary, in NaI these acids prevent particles to uptake liquid water at low RHs, unlike in pure NaI, which admits water at any RH. This retarding effect is especially attributed to OA. In efflorescence, a similar behavior is observed for all systems: the presence of the organic acid makes the particle to retain more water at a given RH, all curves converging at the ERH.

The observed hygroscopic behavior can be due to several factors. Although the morphology of particles can sometimes influence their hygroscopic behavior, all NaX salt dry particles are expected to be cubic, such as NaCl (Fig. 3), as all of them have an octahedral crystal structure. Another possibility is that each organic acid interacts differently with each inorganic salt. Organic acids in the surface of inorganic salts will tend to orientate with their polar groups facing the salt surface, so that ion-dipole interactions will arise that will diminish the system Gibbs free energy. The polarizability of the halogen atoms increases in the order $\text{Cl} (14.7) < \text{Br} (21.8) < \text{I} (35.1)$, all in atomic units (P. Schwerdtfeger, Table of experimental and calculated static dipole polarizabilities for the electronic ground states of the neutral elements, <http://ctcp.massey.ac.nz/dipole-polarizabilities>), so differences in the interaction magnitude are expected. In addition, the surface of particles will become more populated by anions as halide polarizability increases (Jungwirth and Tobias, 2001). Also elongated carbonated chains are known to be easily polarizable. Additionally, it has been proposed that the structure of the monolayers formed with insoluble surfactants determines their resistance towards gas uptake (Stemmler et al., 2008). Fatty acids form a highly ordered film in the so-called liquid condensed state, whereas in the liquid ex-

4397

panded state they form a less ordered film and do not hinder the uptake. In that way, the differences in retardation on water uptake can arise from the different degrees of compression of such films (Donaldson and Vaida, 2006; Takahama and Russell, 2011). Another possibility is that gaseous water transport occurs through open sections of the surface, that can be due to incomplete packing by the organic film or to random fluctuations (Donaldson and Vaida, 2006). The observed salt-specific behavior is in accordance with the observed deliquescent behavior of internally mixed particles formed of sodium halide and water soluble organic acids (Minambres et al., 2011).

The hygroscopic behavior can be correlated with the spectral features of the organic acids shown in Table 2, where the wavenumber and the bandwidth of the C=O band in different environments are shown. The band center wavenumbers shift in the $-6/+10 \text{ cm}^{-1}$ range in the presence of NaX salts, but the bandwidth (FWHM) of the C=O vibration (of $20\text{--}30 \text{ cm}^{-1}$ for the bulk acid) varies in the $-16/+20 \text{ cm}^{-1}$, i.e., a change of more than 100 % in some cases. The wavenumber shift and broadening of a spectral band may arise from a change in the internal force constant of the C=O bond due to the formation of intermolecular bonds with other molecules, for example hydrogen bonds with water (Kalsi, 2007). These results are indicative of the effect of the ionic salt environment near organic acid molecules. Although it is not easy to establish clear correlations with the changes in deliquescence behavior, some remarks can be outlined. For systems with NaBr, the changes in the FWHM of the C=O band are the smallest (except for HA/NaBr), which correlate with a quite small change of DRH (except for HA/NaBr). For NaI mixed with an organic acid, although the changes in FWHM are considerable (indicating strong ion-polar head group interaction), the explanation for the water uptake behavior can be attributed to the hydrophobic effect exerted by the organic acids, forming a barrier that prevents the entrance of gaseous water molecules inside the particles. This effect is very pronounced for NaI/OA, and we have not found a satisfactory explanation for it. Finally, in NaCl/organic acid systems, the opposite effect is observed, in which the presence of acids slightly enhance the entrance of gaseous water. This can be attributed to the ion-polar group interaction that slightly

4398

lowers the Gibbs free energy of the system, favoring the acceptance of gaseous water molecules. The efflorescence process in NaX aqueous particles is not substantially affected by the presence of the acid. As efflorescence is not an activated process, water loss takes place gradually as RH is lowered. Additionally, the salting out effect will make organic acid molecules gradually move out of the surface as the concentration of the salt solution increases. The influence of hexanoic acid on the adsorption of atmospheric gases at the air–water interface has been reported (Demou and Donaldson, 2002). Results indicate a slight increase in the solution-to-surface partitioning of hexanoic acid with increasing salt concentration. NaCl exhibits a “salting-out” effect toward organic species, increasing the surface concentration of organics for fixed solution concentration, but decreasing it for fixed gas-phase concentration. The salting out effect will give rise to an increased surface concentration.

The results on water uptake and release in the special case of HA covered particles give information on how the dynamics of water exchange in inorganic particles is affected by the presence of a surface layer having small water solubility. The evolution of the amounts of liquid HA and water with RH (or, equivalently, the relative amount of gaseous water) in Fig. 5 indicates that, in all deliquescence curves, there is a competition for surface positions between adsorbed HA and gaseous water. Gaseous water tends to displace HA molecules away from the particle surface (as manifested by the reduction in the amount of liquid HA as RH increases), to try to accommodate themselves on the NaX solid surface. This effect must be a consequence of the change in the Gibbs free energy of the system in the deliquescence process: as the energetically most stable system is obtained when gaseous water molecules remain near the solid NaX surface (producing deliquescence when the number of gaseous water molecules reaches a given value), HA molecules will tend to be displaced from their surface locations. In efflorescence, however, the observed behavior is different: removal of water from mixed particles due to the decrease of RH is accompanied by removal of HA from the aqueous particle surface. This effect can be explained assuming that liquid HA uniformly covers the NaX aqueous particle. For water molecules to exit the particles, a

4399

“hole” in the HA layer must be made, and water molecules exiting the particle will sweep away HA molecules from their surface locations. NaX–gaseous water interactions must be stronger in NaCl than in NaBr and NaI or, alternatively, NaX–HA interactions will be weaker for NaCl than for NaBr and NaI. For that reason, in NaX/HA particles, HA is displaced more effectively from the surface at the DRH of pure NaCl. In NaBr and NaI, however, the number density of gaseous water molecules nearby the particles at the DRH of the pure inorganic particle is not enough to remove the HA cover, and a higher number of gaseous water molecules (higher RH) is needed to produce particle deliquescence.

3.5 Estimation of the relative amounts of organic acid and water in the particles

The relative amounts of liquid water and a given organic acid in the aqueous NaX particles can be calculated on average from measured absorbances in their infrared spectra. The number of molecules N_i of a given species i per unit volume of aerosol sample is related with the integrated band absorbance of that species via the Beer–Lambert law (Weis and Ewing, 1996): $\bar{A}_i = \bar{\sigma}_i N_i z / 2.303 \times 10^2$, where \bar{A}_i is the integrated absorbance of a given band (cm^{-1}), $\bar{\sigma}_i$ the integrated absorption cross section per molecule (mmolecule^{-1}) of that band, and z is the optical path length of the aerosol flow cell (m). Applying the previous equation, we can obtain the organic acid/liquid water mole ratio for samples measured in the same aerosol cell, if \bar{A}_i and $\bar{\sigma}_i$ are known: $N_{\text{org}}/N_{\text{H}_2\text{O}} = \bar{A}_{\text{org}}\bar{\sigma}_{\text{H}_2\text{O}}/\bar{A}_{\text{H}_2\text{O}}\bar{\sigma}_{\text{org}}$. The absorption cross section of liquid water has been obtained from pure water data in the $2800\text{--}3600\text{ cm}^{-1}$ range (Downing and Williams, 1975), $\bar{\sigma}_{\text{H}_2\text{O}} = 1.3 \times 10^{-18}\text{ mmolecule}^{-1}$. The absorption cross section for liquid HA and OA have been obtained by measuring the integrated absorbance of a solution of the acid in methanol of known composition in a $150\text{ }\mu\text{m}$ long cell for liquid samples. The C=O band in the $1668\text{--}1774\text{ cm}^{-1}$ range was chosen to compute the integrated absorbance. The obtained values are $\bar{\sigma}_{\text{HA}} = 9.87 \times 10^{-19}\text{ mmolecule}^{-1}$ and $\bar{\sigma}_{\text{OA}} = 1.71 \times 10^{-19}\text{ mmolecule}^{-1}$. From these data, the average $N_{\text{HA}}/N_{\text{H}_2\text{O}}$ and

4400

$N_{\text{OA}}/N_{\text{H}_2\text{O}}$ ratios have been calculated for the various salts at several RHs. The results appear in Fig. 7. The obtained results indicate that $N_{\text{HA}}/N_{\text{H}_2\text{O}}$ values are comprised in the 0.1–0.6 range for RH in the 30–98 % interval, the lowest values corresponding to the highest RHs. In contrast, the $N_{\text{OA}}/N_{\text{H}_2\text{O}}$ quotient spans from 0.2 to 1.9 (for RHs in the 40–96 % range), when again the highest values correspond to the lowest RH conditions. The highest $N_{\text{OA}}/N_{\text{H}_2\text{O}}$ ratio (1.9) is obtained for NaI efflorescing particles. The results in Fig. 7 indicate that, in general, OA-covered particles tend to displace liquid water more efficiently than HA-covered particles.

The spectroscopic results indicate that gaseous HA, OA and LA easily nucleate onto dry and aqueous NaX particles. The amount of acid uptaken increases with the temperature of the oven. Additionally, SEM images of NaCl particles with LA show NaCl particle aggregates, indicating that they are “glued” by lauric acid. However, SEM images provide no visual evidence of the presence of a organic cover, so we can conclude that the cover must be much thinner than the size of the salt particles. A rough higher limit for the cover thickness can be set at 20 nm, which is the resolution of the SEM images. This estimate can be compared with HA and OA cover thickness on aqueous particles, calculated assuming that liquid HA or OA arrange in a hydrophobic organic layer in the surface of an aqueous particle, according to one proposed model (Ellison et al., 1999), and taking into account the spectrally measured relative proportions of water and organic acid. The volume of a spherical aqueous particle of radius R will be $V_{\text{H}_2\text{O}} = (4/3)\pi R^3$, whereas the volume of liquid organic coating of thickness r , assuming uniform coverage, can be written as $V_{\text{org}} = (4/3)\pi[(R + r)^3 - R^3]$. On the other hand, $V_{\text{org}}/V_{\text{H}_2\text{O}} = N_{\text{org}}\rho_{\text{H}_2\text{O}}/(N_{\text{H}_2\text{O}}\rho_{\text{org}})$, where ρ stands for density. As the $N_{\text{org}}/N_{\text{H}_2\text{O}}$ ratios have been determined previously, from the previous equations we can obtain r in terms of the aqueous particle radius R :

$$r/R = [1 + N_{\text{org}}\rho_{\text{H}_2\text{O}}/(N_{\text{H}_2\text{O}}\rho_{\text{org}})]^{1/3} - 1 \quad (1)$$

For typical values of $N_{\text{HA}}/N_{\text{H}_2\text{O}} = 0.1, 0.3$ and 0.6 , $r/R = 0.035, 0.098$ and 0.181 , respectively, indicating that the thickness of the organic layer increases roughly lin-

4401

early with the number of molecules of liquid HA. For example, if $N_{\text{HA}}/N_{\text{H}_2\text{O}} = 0.3$ and $R = 0.3 \mu\text{m}$ (roughly corresponding to NaCl particles appearing in Fig. 3c), the HA coating thickness yields an estimation of $r = 29 \text{ nm}$ for a particle coated with HA. This value can be compared with the upper limit of 20 nm estimated for the cover thickness in the LA/NaCl system. The former HA-coating thickness is much bigger than the estimated thickness of a monolayer, although we cannot affirm whether the particles are uniformly covered. Previous investigations indicate that the degree of insoluble acid coverage do not substantially alter DRH. Complete coverage of inorganic particles by fatty acids had no dramatic effect on NaCl particle DRH (Andrews and Larson, 1993). On the other hand, DRH of ammonium sulfate was only slightly lowered for oleic acid thickness up to 109 nm (Najera and Horn, 2009), much bigger than our estimated thickness of around 30 nm. No variations in DRH with acid covering thickness were observed in this work.

4 Conclusions and atmospheric implications

This work has studied the effect of a covering layer of hexanoic, octanoic and lauric acid, which are present in the Earth's troposphere, on the hygroscopic properties of sodium halide submicrometer particles, which are constituents of sea salt aerosol. Infrared extinction spectroscopy together with particle counting and visualizing techniques has allowed to detect the formation of homogeneously and heterogeneously nucleated particles and the variation of their composition in the presence of variable amounts of gaseous water, leading to the processes of deliquescence and efflorescence. SEM measurements and data deduced from infrared absorbance spectra indicate that the covering thickness of the obtained salt particles is compatible with an average value of 30 nm. SEM images show that the effect of lauric acid on NaCl is to agglomerate salt particles, producing bigger effective particles. It has not been possible to observe this effect with the other acids, due to experimental inconveniences.

It has been found that the hygroscopic properties of sodium halide particles covered with hexanoic, octanoic or lauric acid change both with the nature of the inorganic salt and the carboxylic acid. The DRH of NaCl aerosol is dependent on the organic acid covering the particles, the deliquescence of NaCl/OA and NaCl/LA systems occurring near RH = 56 %, considerably lower than in pure NaCl. On the other hand, NaBr covered particles do not substantially alter their water uptake behavior respect to pure salt particles, irrespective of the organic acid. The growth factor of these particles is also unaffected by the organic coating. Finally, organic acid covering on solid NaI particles act as a barrier to water uptake; non-deliquescenting NaI pure particles deliquesce at about 15 % RH when coated with hexanoic and lauric acid, but the DRH increases remarkably up to 60 % RH for octanoic acid covered particles. The general consequence is that the water uptake behavior of sodium halide particles coated with organic acids can be rather specific. This is in accordance with former studies of sodium halides with succinic acid, which showed a salt-specific behavior. Consequently, although it is customary to extrapolate the water uptake behavior of NaCl particles to sea salt aerosol, due to the predominance of this species in marine salt, the detailed picture can be more complex. Regarding efflorescence process, the obtained results indicate that the overall effect of the organic acid cover is to retain higher amounts of water at RH in the 60–90 % range with respect to pure NaX particles. In NaCl particles the longer chain acid (LA) achieves the highest water retention, the shortest one (HA) producing the lowest. All acids act similarly in NaBr aqueous particles, whereas in aqueous NaI particles OA is the acid that produces higher water retention at RH in the 60–90 % range. The results show that this barrier effect is dependent on the nature of the organic acid, and can have important consequences for the troposphere, as the organic species can determine the amount of liquid water in the particles and their phase at a given RH. Finally, the measurements indicate that there is no simple correlation between water uptake of crystallization processes in coated salt particles and the length of the carbonated chain in the carboxylic acid. The complex behavior in hygroscopic properties in the different salts can not be easily attributed to a single effect, and the results point

4403

to more specific ion-molecule interactions in the NaX/organic acid/H₂O systems or to the structure of the organic film on the particle.

Several consequences for the atmosphere can be driven from this study: as bromine and iodine ions tend to segregate to the surface of marine aerosol particles, and the effect of fatty acids on them can be different as compared to the more abundant NaCl species, this may influence the surface properties of the particles not usually taken into account in the models. At a given value of ambient relative humidity, sea salt particles may have an outer core in which NaBr and NaI are more abundant, and if an organic water insoluble layer is present, the interactions of the organic compound will predominantly take place with bromide and iodide ions. At given conditions of relative humidity in the atmosphere, liquid water amounts and phase of sea-salt particle outer core may vary regard to the expected behavior of pure NaCl particles. This has consequences in the heterogeneous processes taking place between particles and atmospheric gases, such as gas uptake and chemical reactivity.

Acknowledgements. The authors are grateful to Ministerio de Ciencia e Innovación (Madrid) for grant-in-aids (CGL2011-22441 and Consolider CSD-2007-00013), to Gobierno Vasco/Eusko Jaurlaritza (Vitoria-Gasteiz) for a Consolidated Research Group grant (IT520-10), and UPV/EHU for UFI11/23, SEM facilities (SGI/IZO-SGIker) and general support. L.M. thanks UPV/EHU for a postdoctoral research grant. We are grateful to Cristina Gutiérrez from UPV/EHU for the use of the butanol CPC.

References

- Andreae, M. and Rosenfeld, D.: Aerosol–cloud–precipitation interactions. Part 1. The nature and sources of cloud-active aerosols, *Earth-Sci. Rev.*, 89, 13–41, 2008.
- Andrews, E. and Larson, S. M.: Effect of surfactant layers on the size changes of aerosol particles as a function of relative humidity, *Environ. Sci. Technol.*, 27, 857–865, 1993.
- Baker, A. R.: Marine aerosol iodine chemistry: the importance of soluble organic iodine, *Environ. Chem.*, 2, 295–298, 2005.

4404

- Bohren, C. F. and Huffman, D. R.: Absorption and Scattering of Light by Small Particles, Wiley-VCH, Weinheim, 2004.
- Carlsaw, K. S., Boucher, O., Spracklen, D. V., Mann, G. W., Rae, J. G. L., Woodward, S., and Kulmala, M.: A review of natural aerosol interactions and feedbacks within the Earth system, *Atmos. Chem. Phys.*, 10, 1701–1737, doi:10.5194/acp-10-1701-2010, 2010.
- 5 Cavalli, F., Facchini, M. C., Decesari, S., Mircea, M., Emblico, L., Fuzzi, S., Ceburnis, D., Yoon, Y. J., O'Dowd, C. D., Putaud, J. P., and Dell'Acqua, A.: Advances in characterization of size-resolved organic matter in marine aerosol over the North Atlantic, *J. Geophys. Res.-Atmos.*, 109, D24215, doi:10.1029/2004JD005137, 2004.
- 10 Chakraborty, P. and Zachariah, M. R.: Sticking coefficient and processing of water vapor on organic-coated nanoaerosols, *J. Phys. Chem. A*, 112, 966–972, 2008.
- Chuang, P. Y.: Measurement of the timescale of hygroscopic growth for atmospheric aerosols, *J. Geophys. Res.-Atmos.*, 108, 4282, doi:10.1029/2002JD002757, 2003.
- Ciobanu, V. G., Marcolli, C., Krieger, U. K., Weers, U., and Peter, T.: Liquid–liquid phase separation in mixed organic/inorganic aerosol particles, *J. Phys. Chem. A*, 113, 10966–10978, 2009.
- 15 Cwiertrny, D. M., Young, M. A., and Grassian, V. H.: Chemistry and photochemistry of mineral dust aerosol, *Annu. Rev. Phys. Chem.*, 59, 27–51, 2008.
- Davies, J. F., Miles, R. E., Haddrell, A. E., and Reid, J. P.: Influence of organic films on the evaporation and condensation of water in aerosol, *P. Natl. Acad. Sci. USA*, 110, 8807–8812, 2013.
- 20 Demou, E. and Donaldson, D. J.: Adsorption of atmospheric gases at the air–water interface. 4: The influence of salts, *J. Phys. Chem. A*, 106, 982–987, 2002.
- Dennis-Smith, B. J., Hanford, K. L., Kwamena, N. A., Miles, R. E. H., and Reid, J. P.: Phase, morphology, and hygroscopicity of mixed oleic acid/sodium chloride/water aerosol particles before and after ozonolysis, *J. Phys. Chem. A*, 116, 6159–6168, 2012.
- 25 Donaldson, D. J. and Vaida, V.: The influence of organic films at the air–aqueous boundary on atmospheric processes, *Chem. Rev.*, 106, 1445–1461, 2006.
- Downing, H. D. and Williams, D.: Optical constants of water in the infrared, *J. Geophys. Res.*, 80, 1656–1661, 1975.
- 30 Duce, R., Mohnen, V., Zimmerman, P., Grosjean, D., Cautreels, W., Chatfield, R., Jaenicke, R., Ogren, J., Pellizzari, E., and Wallace, G.: Organic material in the global troposphere, *Rev. Geophys.*, 21, 921–952, 1983.

4405

- Ebben, C. J., Ault, A. P., Ruppel, M. J., Ryder, O. S., Bertram, T. H., Grassian, V. H., Prather, K. A., and Geiger, F. M.: Size-resolved sea spray aerosol particles studied by vibrational sum frequency generation, *J. Phys. Chem. A*, 117, 6589–6601, 2013.
- Ellison, G. B., Tuck, A. F., and Vaida, V.: Atmospheric processing of organic aerosols, *J. Geophys. Res.-Atmos.*, 104, 11633–11641, doi:10.1029/1999JD900073, 1999.
- 5 Finlayson-Pitts, B. J.: The tropospheric chemistry of sea salt: a molecular-level view of the chemistry of NaCl and NaBr, *Chem. Rev.*, 103, 4801–4822, 2003.
- Finlayson-Pitts, B. J.: Reactions at surfaces in the atmosphere: integration of experiments and theory as necessary (but not necessarily sufficient) for predicting the physical chemistry of aerosols, *Phys. Chem. Chem. Phys.*, 11, 7760–7779, 2009.
- 10 Freney, E. J., Martin, S. T., and Buseck, P. R.: Deliquescence and efflorescence of potassium salts relevant to biomass-burning aerosol particles, *Aerosol Sci. Tech.*, 43, 799–807, 2009.
- Frinak, E. K. and Abbatt, J. P. D.: Br(2) production from the heterogeneous reaction of gas-phase OH with aqueous salt solutions: impacts of acidity, halide concentration, and organic surfactants, *J. Phys. Chem. A*, 110, 10456–10464, 2006.
- 15 Gadermann, M., Preston, T. C., Troster, C., and Signorell, R.: Characterization of palmitic and lauric acid aerosols from rapid expansion of supercritical CO₂ solutions, *Mol. Phys.*, 106, 945–953, 2008.
- Gantt, B. and Meskhidze, N.: The physical and chemical characteristics of marine primary organic aerosol: a review, *Atmos. Chem. Phys.*, 13, 3979–3996, doi:10.5194/acp-13-3979-2013, 2013.
- 20 Garland, R. M., Wise, M. E., Beaver, M. R., DeWitt, H. L., Aiken, A. C., Jimenez, J. L., and Tolbert, M. A.: Impact of palmitic acid coating on the water uptake and loss of ammonium sulfate particles, *Atmos. Chem. Phys.*, 5, 1951–1961, doi:10.5194/acp-5-1951-2005, 2005.
- 25 Ghosal, S., Brown, M. A., Bluhm, H., Krisch, M. J., Salmeron, M., Jungwirth, P., and Hemminger, J. C.: Ion partitioning at the liquid/vapor interface of a multicomponent alkali halide solution: a model for aqueous sea salt aerosols, *J. Phys. Chem. A*, 112, 12378–12384, 2008.
- Gill, P., Graedel, T., and Weschler, C.: Organic films on atmospheric aerosol particles, fog droplets, cloud droplets, raindrops, and snowflakes, *Rev. Geophys.*, 21, 903–920, 1983.
- 30 Hämeri, K., Rood, M., and Hansson, H.: Hygroscopic properties of a NaCl aerosol coated with organic compounds, *J. Aerosol Sci.*, 23, 437–440, 1992.

4406

- Hansson, H. C., Rood, M. J., Koloutsou-Vakakis, S., Hameri, K., Orsini, D., and Wiedensohler, A.: NaCl aerosol particle hygroscopicity dependence on mixing with organic compounds, *J. Atmos. Chem.*, 31, 321–346, 1998.
- Hayase, S., Yabushita, A., Kawasaki, M., Enami, S., Hoffmann, M. R., and Colussi, A. J.: Weak acids enhance halogen activation on atmospheric water's surfaces, *J. Phys. Chem. A*, 115, 4935–4940, 2011.
- Hinds, W. C.: *Aerosol Technology: Properties, Behavior, and Measurement of Airborne Particles*, John Wiley & Sons, Los Angeles, California, 1998.
- Hunt, S. W., Roeselova, M., Wang, W., Wingen, L. M., Knipping, E. M., Tobias, D. J., Dabdub, D., and Finlayson-Pitts, B. J.: Formation of molecular bromine from the reaction of ozone with deliquesced NaBr aerosol: evidence for interface chemistry, *J. Phys. Chem. A*, 108, 11559–11572, 2004.
- Jungwirth, P. and Tobias, D. J.: Molecular structure of salt solutions: a new view of the interface with implications for heterogeneous atmospheric chemistry, *J. Phys. Chem. B*, 105, 10468–10472, 2001.
- Krueger, B. J., Grassian, V. H., Iedema, M. J., Cowin, J. P., and Laskin, A.: Probing heterogeneous chemistry of individual atmospheric particles using scanning electron microscopy and energy-dispersive X-ray analysis, *Anal. Chem.*, 75, 5170–5179, 2003.
- Kwamena, N.-A., Buajarn, J., and Reid, J. P.: Equilibrium morphology of mixed organic/inorganic/aqueous aerosol droplets: investigating the effect of relative humidity and surfactants, *J. Phys. Chem. A*, 114, 5787–5795, 2010.
- Lewis, R. and Schwartz, E.: *Sea salt aerosol production: mechanisms, methods, measurements and models – a critical review*, American Geophysical Union, Washington, 2004.
- Li, H.: *Refractive index of alkali halides and its wavelength and temperature derivatives*, American Chemical Society, Indiana, 1976.
- Ma, X., Chakraborty, P., Henz, B. J., and Zachariah, M. R.: Molecular dynamic simulation of dicarboxylic acid coated aqueous aerosol: structure and processing of water vapor, *Phys. Chem. Chem. Phys.*, 13, 9374–9384, 2011.
- Martin, S. T.: Phase transitions of aqueous atmospheric particles, *Chem. Rev.*, 100, 3403–3453, 2000.
- Metzger, S. and Lelieveld, J.: Reformulating atmospheric aerosol thermodynamics and hygroscopic growth into fog, haze and clouds, *Atmos. Chem. Phys.*, 7, 3163–3193, doi:10.5194/acp-7-3163-2007, 2007.

4407

- Middlebrook, A. M., Murphy, D. M., and Thomson, D. S.: Observations of organic material in individual marine particles at Cape Grim during the First Aerosol Characterization Experiment (ACE 1), *J. Geophys. Res.*, 103, 16475–16483, 1998.
- Mikhailov, E., Vlasenko, S., Rose, D., and Pöschl, U.: Mass-based hygroscopicity parameter interaction model and measurement of atmospheric aerosol water uptake, *Atmos. Chem. Phys.*, 13, 717–740, doi:10.5194/acp-13-717-2013, 2013.
- Minambres, L., Sanchez, M. N., Castano, F., and Basterretxea, F. J.: Infrared spectroscopic properties of sodium bromide aerosols, *J. Phys. Chem. A*, 112, 6601–6608, 2008.
- Minambres, L., Sanchez, M. N., Castano, F., and Basterretxea, F. J.: Hygroscopic properties of internally mixed particles of ammonium sulfate and succinic acid studied by infrared spectroscopy, *J. Phys. Chem. A*, 114, 6124–6130, 2010.
- Minambres, L., Mendez, E., Sanchez, M. N., Castano, F., and Basterretxea, F. J.: Water uptake properties of internally mixed sodium halide and succinic acid particles, *Atmos. Environ.*, 45, 5896–5902, 2011.
- Mochida, M., Kitamori, Y., Kawamura, K., Nojiri, Y., and Suzuki, K.: Fatty acids in the marine atmosphere: factors governing their concentrations and evaluation of organic films on sea-salt particles, *J. Geophys. Res.-Atmos.*, 107, 4325, doi:10.1029/2001JD001278, 2002.
- Najera, J. J. and Horn, A. B.: Infrared spectroscopic study of the effect of oleic acid on the deliquescence behaviour of ammonium sulfate aerosol particles, *Phys. Chem. Chem. Phys.*, 11, 483–494, 2009.
- O'Dowd, C. D. and De Leeuw, G.: Marine aerosol production: a review of the current knowledge, *Philos. T. Roy. Soc. A*, 365, 1753–1774, 2007.
- Prather, K. A., Bertram, T. H., Grassian, V. H., Deane, G. B., Stokes, M. D., DeMott, P. J., Aluwihare, L. I., Palenik, B. P., Azam, F., and Seinfeld, J. H.: Bringing the ocean into the laboratory to probe the chemical complexity of sea spray aerosol, *P. Natl. Acad. Sci. USA*, 110, 7550–7555, 2013.
- Quinn, P. and Bates, T.: The case against climate regulation via oceanic phytoplankton sulphur emissions, *Nature*, 480, 51–56, 2011.
- Reid, J. P., Dennis-Smith, B. J., Kwamena, N. A., Miles, R. E., Hanford, K. L., and Homer, C. J.: The morphology of aerosol particles consisting of hydrophobic and hydrophilic phases: hydrocarbons, alcohols and fatty acids as the hydrophobic component, *Phys. Chem. Chem. Phys.*, 13, 15559–15572, 2011.




4408

- Robinson, C. B., Schill, G. P., Zarzana, K. J., and Tolbert, M. A.: Impact of organic coating on optical growth of ammonium sulfate particles, *Environ. Sci. Technol.*, 47, 13339–13346, 2013.
- Rossi, M. J.: Heterogeneous reactions on salts, *Chem. Rev.*, 103, 4823–4882, 2003.
- 5 Rubasinghege, G., Ogden, S., Baltrusaitis, J., and Grassian, V. H.: Heterogeneous uptake and adsorption of gas-phase formic acid on oxide and clay particle surfaces: the roles of surface hydroxyl groups and adsorbed water in formic acid adsorption and the impact of formic acid adsorption on water uptake, *J. Phys. Chem. A*, 117, 11316–11327, 2013.
- Saiz-Lopez, A., Mahajan, A. S., Salmon, R. A., Bauguitte, S. J., Jones, A. E., Roscoe, H. K.,
10 and Plane, J. M. C.: Boundary layer halogens in coastal Antarctica, *Science*, 317, 348–351, 2007.
- Soule, M. C. K., Blower, P. G., and Richmond, G. L.: Effects of atmospherically important solvated ions on organic acid adsorption at the surface of aqueous solutions, *J. Phys. Chem. B*, 111, 13703–13713, 2007.
- 15 Stemmler, K., Vlasenko, A., Guimbaud, C., and Ammann, M.: The effect of fatty acid surfactants on the uptake of nitric acid to deliquesced NaCl aerosol, *Atmos. Chem. Phys.*, 8, 5127–5141, doi:10.5194/acp-8-5127-2008, 2008.
- Sun, L., Hede, T., Tu, Y., Leck, C., and Ågren, H.: Combined effect of glycine and sea salt on aerosol cloud droplet activation predicted by molecular dynamics simulations, *J. Phys. Chem. A*, 117, 10746–10752, 2013.
- 20 Sun, L., Li, X., Hede, T., Tu, Y., Leck, C., and Ågren, H.: Molecular dynamics simulations of the surface tension and structure of salt solutions and clusters, *J. Phys. Chem. B*, 116, 3198–3204, 2012.
- Tabazadeh, A.: Organic aggregate formation in aerosols and its impact on the physicochemical properties of atmospheric particles, *Atmos. Environ.*, 39, 5472–5480, 2005.
- 25 Takahama, S. and Russell, L.: A molecular dynamics study of water mass accommodation on condensed phase water coated by fatty acid monolayers, *J. Geophys. Res.-Atmos.*, 116, D02203, doi:10.1029/2010JD014842, 2011.
- Tervahattu, H., Hartonen, K., Kerminen, V. M., Kupiainen, K., Aarnio, P., Koskentalo, T.,
30 Tuck, A. F., and Vaida, V.: New evidence of an organic layer on marine aerosols, *J. Geophys. Res.-Atmos.*, 107, 4053, doi:10.1029/2000JD000282, 2002.
- Veghte, D. P., Altaf, M. B., and Freedman, M. A.: Size dependence of the structure of organic aerosol, *J. Am. Chem. Soc.*, 135, 16046–16049, 2013.

4409

- Von Glasow, R.: Atmospheric chemistry – sun, sea and ozone destruction, *Nature*, 453, 1195–1196, 2008.
- Wagner, J., Andrews, E., and Larson, S. M.: Sorption of vapor phase octanoic acid onto deliquescent salt particles, *J. Geophys. Res.*, 101, 19533–19540, 1996.
- 5 Weis, D. D. and Ewing, G. E.: Infrared spectroscopic signatures of $(\text{NH}_4)_2\text{SO}_4$ aerosols, *J. Geophys. Res.*, 101, 18709–18720, 1996.
- Wise, M. E., Baustian, K. J., Koop, T., Freedman, M. A., Jensen, E. J., and Tolbert, M. A.: Depositional ice nucleation onto crystalline hydrated NaCl particles: a new mechanism for ice formation in the troposphere, *Atmos. Chem. Phys.*, 12, 1121–1134, doi:10.5194/acp-12-1121-2012, 2012.
- 10 Zangmeister, C. D., Turner, J. A., and Pemberton, J. E.: Segregation of NaBr in NaBr/NaCl crystals grown from aqueous solutions: implications for sea salt surface chemistry, *Geophys. Res. Lett.*, 28, 995–998, doi:10.1029/2000GL012539, 2001.

Table 1. Physical properties of the studied carboxylic acids.

Name	#C	Structural Formula	Melting Point (K) ^a	Boiling Point (K) ^a	Vapour pressure (mm Hg, 25 °C) ^b
Hexanoic Acid	6		269.7	477 ± 4	0.2
Octanoic Acid	8		289.3 ± 0.7	510 ± 4	3.71 × 10 ⁻³
Lauric Acid	12		317 ± 2	571	1.6 × 10 ⁻⁵

^a NIST Chemistry WebBook.^b PubChem Compound, NCBI (National Centre for Biotechnology Information).

4411

Table 2. Band position and bandwidth of the C=O stretching band in various conditions for HA, OA and LA. Units in cm⁻¹.

	Hexanoic acid		Octanoic acid		Lauric acid	
	Wavenumber at maximum intensity	Bandwidth (FWHM)	Wavenumber at maximum intensity	Bandwidth (FWHM)	Wavenumber at maximum intensity	Bandwidth (FWHM)
gas ^a	1780	26	1780	62	1790	30
bulk	1710	20	1713	26	1700	29
homog. nucl.	1730	26	1700	46	1710	21
heter. NaCl ^b	1717	27–40 ^c	1707	19	1710	19
heter. NaBr ^b	1711–1720 ^c	27–37 ^c	1713	23	1708	26
heter. NaI ^b	1720	33	1713	36	1707	13

^a NIST Chemistry Webbook: <http://webbook.nist.gov/chemistry>.^b Dry particles.^c Depending on the amount of acid deposited onto the salt particles.

4412

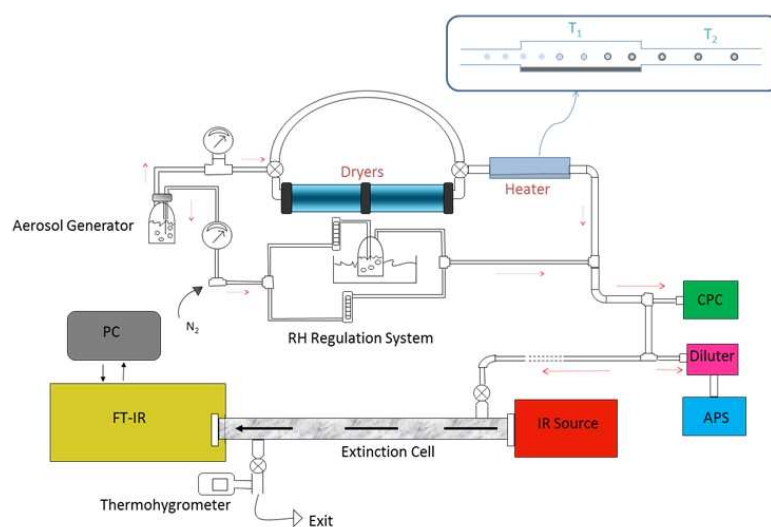


Fig. 1. Diagram of the experimental setup.

4413

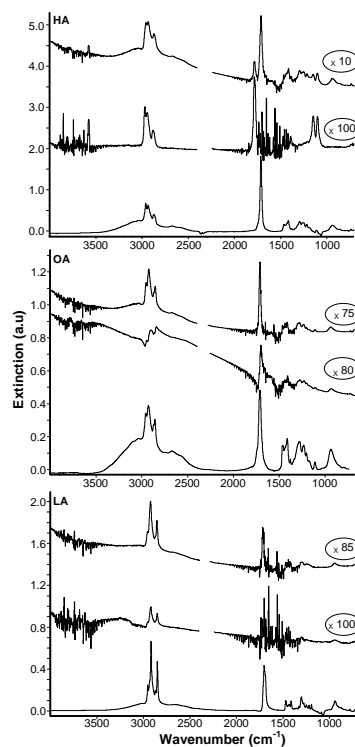


Fig. 2. Infrared extinction spectra of HA, OA and LA in different conditions: bottom spectra are from bulk phase acid; medium spectra corresponds to homogeneously nucleated acid particles; upper spectra are from heterogeneously nucleated acids onto NaCl particles.

4414

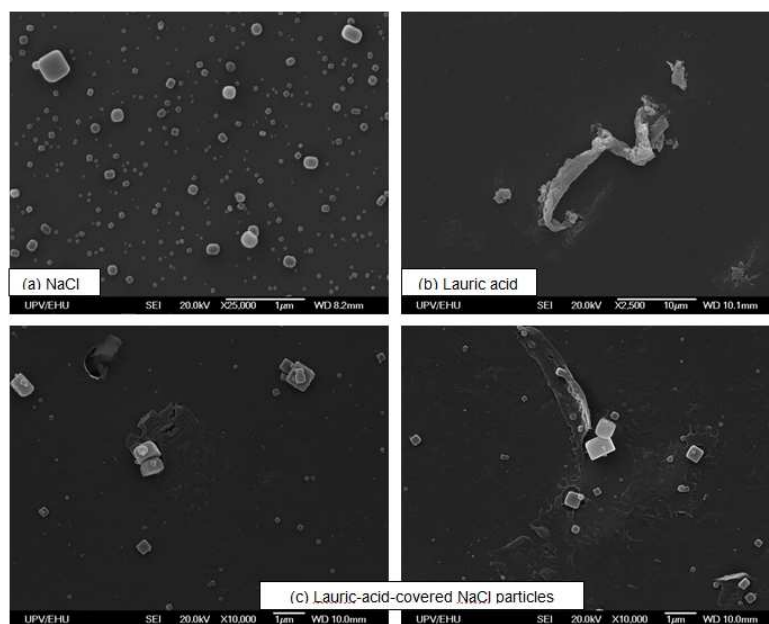


Fig. 3. SEM images of: **(a)** pure NaCl particles; **(b)** pure LA particles; **(c)** NaCl particles covered with LA.

4415

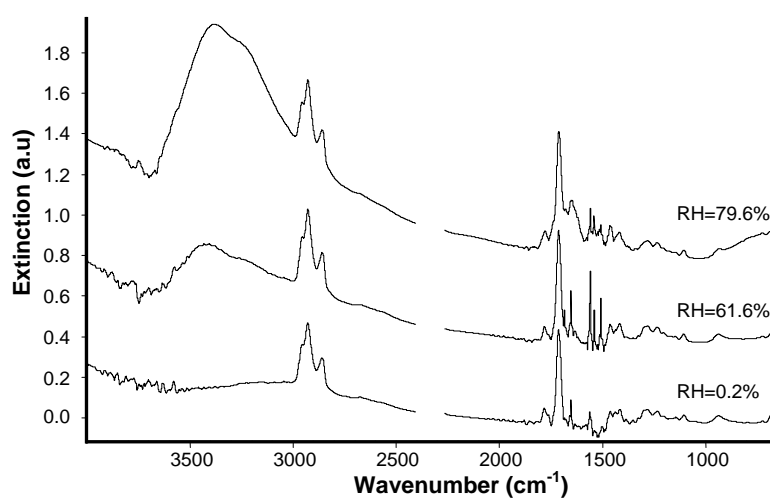


Fig. 4. Infrared spectra of NaBr particles after passing through the heated reservoir containing OA and exposed to different RHs.

4416

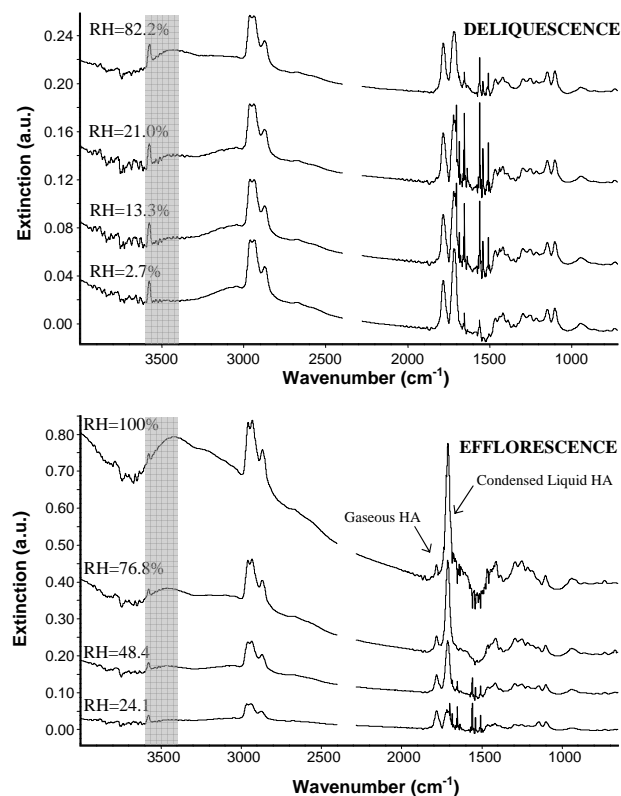


Fig. 5. Evolution of the infrared absorption intensity of the C=O band of hexanoic acid with RH in NaBr particles in deliquescence and efflorescence mode. The shaded region indicates the selected area for measuring liquid water abundance in the particles (see text).

4417

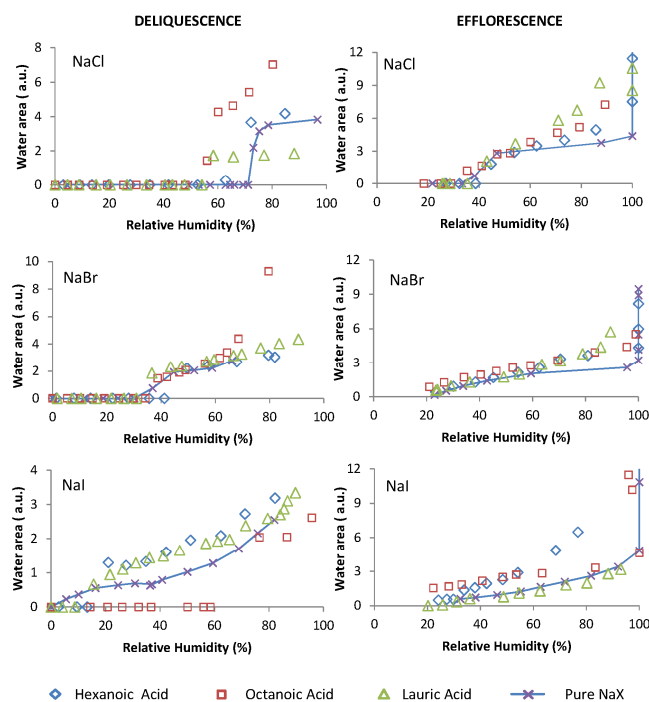


Fig. 6. Deliquescence and efflorescence curves of NaX (X = Cl, Br, I) particles covered with HA, OA and LA. The curves for the pure inorganic salts are shown by lines.

4418

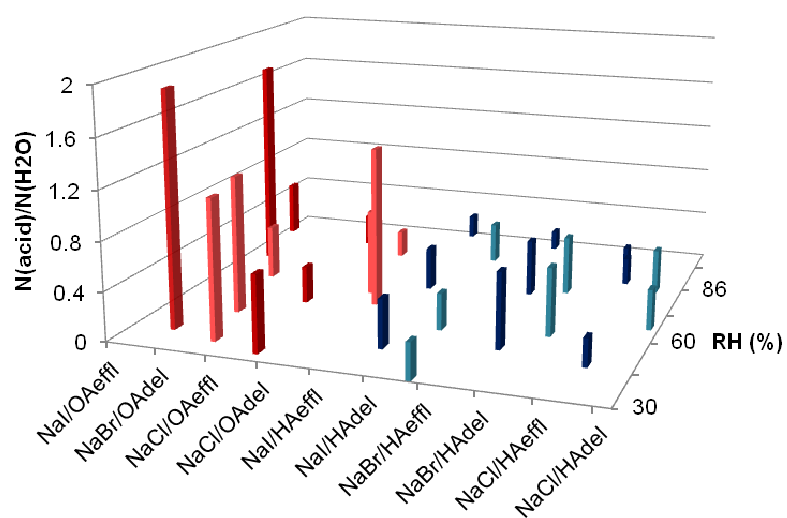


Fig. 7. $N_{\text{HA}}/N_{\text{H}_2\text{O}}$ and $N_{\text{OA}}/N_{\text{H}_2\text{O}}$ mole ratios in heterogeneously coated particles at various relative humidities in deliquescence and efflorescence conditions. “del” and “effl” stand for deliquescence and efflorescence. “RH” stands for relative humidity.